Received 25 April 2023; revised 4 July 2023; accepted 10 August 2023. Date of publication 29 August 2023; date of current version 18 September 2023. The review of this article was arranged by Associate Editor Mauro Di Nardo.

Digital Object Identifier 10.1109/OJIA.2023.3309627

Development of Polymer-Ceramic Composite Materials for the Winding Insulation of Highly Utilized and Energy-Efficient Electrical Machines

SÖREN MIERSCH [1], RALPH SCHUBERT [2], THOMAS SCHUHMANN [1] (Member, IEEE), AND MATHIAS LINDNER [3]

[1]Faculty Electrical Engineering, University of Applied Sciences Dresden, 01069 Dresden, Germany
[2]Polymerceramic Composites, Fraunhofer Institute for Ceramic Technologies and Systems IKTS, 07629 Hermsdorf, Germany
[3]IAV GmbH, 09366 Stollberg, Germany

CORRESPONDING AUTHOR: SÖREN MIERSCH (e-mail: soeren.miersch@htw-dresden.de)

This work was supported in part by the Industrial Collective Research from Consortium of Industrial Research Associations, in part by the German Federal Ministry of Economic Affairs and Climate Action, in part by the Open Access Publication Fund of University of Applied Sciences Dresden, and in part by DFG German Research Foundation under Grant 491382348.

ABSTRACT The electromagnetic utilization of an electrical machine can be increased by raising the current density, with a limitation resulting from the maximum permissible temperature of the winding insulation. Conventional insulating materials only have a low specific thermal conductivity, which results in large temperature gradients in the winding cross section and consequently hotspots. This article presents the development and characterization of ceramic-like composite materials based on filled polysiloxanes for the dip coating of lamination stacks and the impregnation of the winding of electrical machines. The specific equivalent thermal conductivity is determined on composite winding samples, the thermal cycle stability is examined and the microstructure is analyzed with the scanning electron microscope. The manufacturability and the partial discharge behavior are examined based on test samples. The results of tests on an electric traction machine are used to show the potential for increasing the power density.

INDEX TERMS Ceramic insulation, electric machines, impregnated insulation, machine windings, thermal variables measurement.

I. INTRODUCTION

The challenges of a transition towards renewable energy systems result in increasing requirements for the design of electrical machines. On the one hand, these should be energy-efficient. On the other hand, especially for mobile applications as in the area of electric mobility and electric aircraft, they should offer a high-power density, which is synonymous with improved resource efficiency. A higher power density can be achieved by increasing the linear current density (i.e., the magnetomotive force per length), the air gap induction or the mechanical speed [1], [2], [3], [4]. The air gap induction is limited to values of about 1.1 T due to the saturation of the magnetic circuit. Speed increases that cause circumferential speeds of the rotor of >150 m/s are mechanically challenging. In this case, the use of carbon fiber bandages, high-strength electrical steel, or special copper alloys in the squirrel cage of induction machines are necessary [5], [6], [7], [8]. The only remaining possibility is increasing the linear current density, but this requires intensified cooling of the windings [1], [2], [3], [4].

For the winding insulation of electrical machines with a rated voltage <1 kV, insulating sheets are applied as the main or interphase insulation. The winding itself consists of mutually insulated enameled copper wires. It is impregnated with the aim of avoiding air inclusions or even fully encapsulated including the end windings. Conventional insulating materials generally have a low specific thermal conductivity of around 0.2 W/(m·K). As the machine load increases, this results in large temperature gradients in the winding cross section and consequently hotspots. With regard to the thermal rating of the insulating materials, the electromagnetic utilization of the machines must be limited. Cooling methods such as direct cooling of the conductors or the approach of applying ceramic-like winding insulation for electrical machines presented in this article allow shifting this limitation to higher levels.

II. INSULATION MATERIALS AND PROCESSES

A. STATE OF THE ART–INSULATION MATERIALS AND PROCESSES

At present, the main insulation of the winding or the lamination stack of electrical machines with a rated voltage <1 kV is primarily implemented using insulating sheet materials such as polyester film and polyester fleece. The thickness of those materials is typically (0.1 …0.4) mm, the specific thermal conductivities are in the range of (0.1 …0.2) W/(m·K). For fractional horsepower machines, the plastic coating of lamination stacks or single teeth offers an alternative. However, the layer thicknesses exceed 0.4 mm due to the solidification process; the specific thermal conductivity of the applied plastic materials is approximately 0.2 W/(m·K). The maximum permissible temperature of the aforementioned materials is usually below 220 °C; thermal class "H" with $\vartheta_{\max} = 180$ °C is typical for applications in the field of electric mobility.

When impregnating the windings of electrical machines, dipping, hot-dipping, dip-rolling, trickling, or vacuum-pressure impregnation processes are used. High impregnation factors (i.e., avoidance of air inclusions) can be achieved particularly in the vacuum pressure impregnation process. The impregnating or soaking materials used are low-viscous (viscosity in the range (100...1000) mPa·s), hydrocarbon-based synthetic resins based on polyester, polyamide, polyesterimide, epoxide, polyurethane, phenol, or melamine. They typically have a specific thermal conductivity of (0.15 …0.2) W/(m·K), can withstand temperatures of up to 220 °C and, in the cross-linked state, ensure high mechanical strength of the winding composite. The impregnating materials are generally unfilled and consist of one component. In some cases, solvents such as styrene, which is flammable and harmful to health, are added with the aim of improving the impregnation result.

For potting the windings of electrical machines, e.g., for connecting the end windings to the cooling system or for full encapsulation of the stator, mineral-filled encapsulation compounds based on epoxy, polyurethane, polyesterimide, or silicone are used [9], [10], [11]. The casting compounds are usually applied as a two-component system. Depending on the degree of filling, the specific thermal conductivity is (0.5 …2.5) W/(m·K) and the thermal rating is usually below 220 °C (special casting compounds reach up to 250 °C). Only low-viscous systems (with a mixed viscosity in the range (1500 …3000) mPa·s), which have specific thermal conductivities of up to 0.6 W/(m·K) with a low filling level, are suitable for fully potting the windings of electrical machines with round and profile wire winding. Potting under vacuum is preferred to avoid air inclusions.

B. STATE OF RESEARCH–CERAMIC-LIKE INSULATION OF ELECTRICAL MACHINES

With the aim of increasing power density and therewith reducing active mass (i.e., enhancing resource efficiency), a clear trend towards high temperature-stable and better thermally conductive insulating materials can be seen in the technology fields of electric mobility and electric aircraft. In this regard, Kulan et al. [12] give a comprehensive overview of the developments. In [13], it is shown that by coating copper wires with aluminum oxide Al_2O_3, the thermal conductivity of the winding composite can be increased by a factor of approximately 2.5, with an epoxy resin being used as the impregnating material. Such wire coatings are currently of increasing interest for high-temperature applications in the aerospace sector, whereby the mechanical and electrical load capacity is still limited due to the brittleness of the ceramics [14], [15], however. In addition to Cu/Ni wires [16], [17], [18], development is currently also focusing on thermal spray coating with Al_2O_3 [19]. There are also initial approaches to electrochemical coating of lamination stacks, with thermal conductivities of the insulation of up to 2 W/(m·K) and temperature stability of up to 300 °C being achieved [20]. The filling of polymer materials with ceramic fillers to improve the specific thermal conductivity is known, with thermal conductivities of up to approximately 2.5 W/(m·K) being achievable with high levels of filling [21], [22], [23]. In [24], [25], [26], and [27], the use of ceramic fillers is examined for high-voltage machines up to a filling level of 25 vol.-%, which doubles the thermal conductivity of the impregnating material from 0.3 W/(m·K) to 0.6 W/(m·K). As such, the excess temperature of the winding can be reduced by approximately 10 K. With regard to the high temperature resistant and thermally conductive insulation of electrical machines with a rated voltage <1 kV containing round and profile wire windings, there is still a great need for development. In this regard, the development approach for ceramic-filled polysiloxanes presented in this article makes a contribution (cf., [28], [29], [30], [31]).

III. MATERIAL DEVELOPMENT AND CHARACTERIZATION

A. DEVELOPMENT OF COMPOSITE MATERIALS

In this article, composite materials have been developed for the winding impregnation and the main insulation of lamination stacks. They consist of a polysiloxane matrix and ceramic fillers. The matrix is created through the thermal cross-linking of liquid silicone resins, with the selection of suitable reactive centers enabling the formation of dense and pore-free composite structures. Aluminum oxide (α-Al_2O_3), aluminum nitride (AlN), and boron nitride (α-BN) were used as fillers.

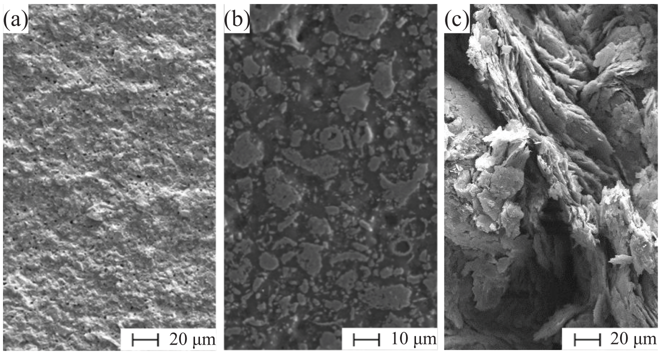

FIGURE 1. **Microstructure of the composite systems with the fillers. (a) Al_2O_3. (b) AlN. (c) BN.**

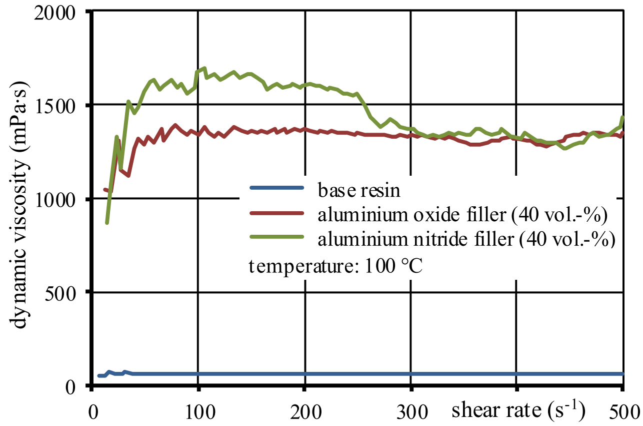

FIGURE 2. **Characterization of dynamic viscosity of the composite materials with rotational viscosimeter.**

The fillers based on aluminum compounds have grain sizes in the range of (2...6) μm and their surfaces have been pretreated with a hydrophobic coating process described in [32] in order to ensure high filling levels without impairing the flowability of the composite. Boron nitride was used as pregranulate with an average grain size of 30 μm without further pretreatment.

Composites with a flowability suitable for the impregnation of winding systems could be filled with up to 40 vol.-% filler when using Al_2O_3 or AlN. For comparison, boron nitride-filled systems were produced with a filler content of up to 30 vol.-% and did not exhibit suitable impregnation behavior overall. The impregnation or coating systems were produced by stirring the components at 80 °C and showed no tendency to separate even after several days. Mixing was followed by repeated degassing at 120 °C under vacuum (100 mbar). The systems pretreated in this way had a flowability at temperatures above 140 °C suitable for dip impregnation or coating without vacuum. The matrix crosslinking took place at 180 °C for 8 h under normal pressure.

B. CHARACTERIZATION OF MATERIAL PROPERTIES

1) MEASURING METHODS AND MATERIAL CHARACTERIZATION

Investigation of microstructure of the composites for impregnation and main insulation with a field emission raster electron microscope Ultra 55 plus (Zeiss) revealed a smooth integration of the AlN and Al_2O_3 filler components into the polymer matrix. The boron nitride filler behaves differently. Here, the big grain size, the platelet structure, and the special surface interfere a wetting with the matrix polymer and a more even powder distribution in the composite matrix (cf., Fig. 1).

To characterize the flowability of the composite systems, their viscosity was determined using the *HAAKE Viscotester 550 rotational viscometer* with a plate-plate configuration and a gap distance of 0.25 mm. Measurements of the unfilled matrix resin system as well as the AlN or Al_2O_3-filled systems at shear rates, which are comparable to the processing conditions in stator production in the range of $(0\ldots500)\ s^{-1}$, and a material temperature of 100 °C show a strong increase in viscosity due to the filling. A largely independent viscosity from the shear rate of the unfilled and Al_2O_3-filled system indicates a flow behavior of an ideal Newtonian liquid. In the AlN-filled system, the viscosity decreases abruptly at a shear rate of 250 s^{-1}, which can be interpreted as the destruction of internal flow-inhibiting structures (cf., Fig. 2). This is contradicted by the fact that the two fillers Al_2O_3 and AlN have comparable morphologies with almost round grain shapes. BN-filled systems with a degree of filling of 30 vol.-%, which is sufficient to increase the thermal conductivity, showed such a low flowability that their viscosity could not be measured with the selected measuring method.

The three-point flexural strength according to DIN EN 843-1 was measured using the *TIRAtest 2300* measuring device from the *Rauenstein Franz Wohl and Partner Prüfmaschinen GmbH* with a 1 kN pressure sensor and a driving speed of 100 mm/s. Cast bars with dimension of $(5\times5\times50)\ mm^3$ were used as test specimens.

The linear thermal expansion coefficient of the developed composite materials was characterized with *NETZSCH* thermo-mechanical analyzer *TMA 402F3*. The measuring principle is based on a highly precise inductive displacement transducer. The measurements were carried out in nitrogen in a temperature range of $(20\ldots200)$ °C with a heating rate of 5 K/min.

The thermal conductivity of the pure composite materials was determined using the *TPS 2500 S* measuring device from *Hot Disk AB*. The measuring principle is based on the transient plane source technique (TPS). This technique, also known as the hot-disk method, works dynamically in a non-stationary manner, whereby heat is introduced through a flat and round heater into two material samples that are arranged tightly below and above the heater (cf., Fig. 3). A resistance thermocouple is integrated in the heating element, which enables the temperature to be determined as a function of the measuring time. The temperature measurement begins after an initial period for the heater to heat up and for the heat to be coupled into the specimen and must be completed before the heat front reaches the specimen edges. Plates measuring $(20\times20\times5)\ mm^3$ proved to be suitable for determining the

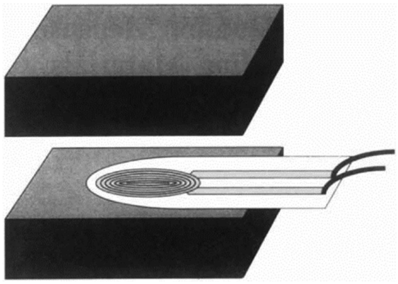

FIGURE 3. Principal setup for the measurement of thermal conductivity by TPS method [33].

TABLE 1. Realized Properties of Polymer-Ceramic Composite Materials for Winding Insulation

Property	Method	Impregnation / Coating		
filler		Al_2O_3	AlN	BN
filling degree (vol.-%)		40	40	30
viscosity (mPa·s)	DIN 53019-1	1300	1600	-
flexural strength (MPa)	DIN EN 843-1	35.6	19.2	31.8
coefficient of thermal expansion (ppm/K)	ISO 11359-2	127	100	131
thermal conductivity (W/(m·K))	ISO 22007-2	0.83	1.16	2.76
specific electrical resistance (10^{15} Ω·cm)	DIN EN 62631-3-1	4.23	6.64	0.28
dielectric strength (kV/mm)	DIN EN 60243-1	25.1	23.1	20.2

thermal conductivity of the composite materials. The thermal conductivity and the thermal diffusivity can be determined from the recorded temperature-time curves. The method only provides reliable measurement values if the specimens have sufficient isotropy so that the heat coupled into the specimen can spread evenly in all spatial directions [33].

The specific electrical resistance according to DIN EN 62631-3-1 was determined using a milli- and teraohmmeter *Milli-TO3* from *Fischer Elektronik*. Cast samples with dimensions of $(100\times100\times1)$ mm^3 were used, which were printed with silver electrodes for contacting. The tests were carried out with measuring voltages in the range of (10 …500) V dc at 23 °C and a relative humidity of 50 %.

The determination of the dielectric strength according to DIN EN 60243-1 was carried out with the high-voltage test device *HV-Control* from *H+H High-Voltage Technology GmbH*. Cast samples with dimensions of $(100\times100\times1)$ mm^3, which were printed with copper electrodes, were used. The measurements were carried out with test voltages of up to 130 kV dc.

2) SUMMARY OF MATERIAL PROPERTIES

Table 1 summarizes the main processing and application-relevant properties of the polysiloxane-based composite materials developed for winding impregnation and main insulation.

TABLE 2. Preliminary Estimation of the Price for the Composite Systems

Filler	Filling degree (vol.-%)	Mass percentage (ma.-%)	Price (€/kg)
AlN	40	64	80
Al_2O_3	40	68	15
BN	30	45	63

The AlN or Al_2O_3-filled systems have sufficient flowability for dip impregnation or coating at filling levels of up to 40 vol.-%. In addition, these systems exhibit a thermal conductivity up to five times higher than classic impregnation systems such as polyesters and epoxides, and comparable electrical insulation properties. Although the BN-filled systems have an even better thermal conductivity, their development was not continued due to the insufficient flow properties.

With regard to the subsequent application for the insulation of electrical machines, the developed materials are subject to different pressures on prices depending on the industrial sector. Commonly used epoxy resins are in the range (6 …10) €/kg. A significantly larger price range of (15 …60) €/kg can be found for filled potting compounds that are used for full stator potting, though they are not suitable for winding impregnation due to their rheological properties. For the raw materials used, there are the following rough guiding prices: AlN approximately 100 €/kg (laboratory supply < 5 kg), Al_2O_3 in the range (0.5 …1.4) €/kg (industry supply > 1 t, depending on granule pretreatment), BN approximately 85 €/kg (industry supply approximately 50 kg), and silicone resin with possible industrial price of approximately 45 €/kg. As a preliminary estimate, the prices listed in Table 2 result for the composite systems discussed, although these will be further reduced by increasing industrial application. The proportion of impregnating agent in the winding of a traction machine in the double-digit kilowatt range is around 1 kg. With the increase in electromagnetic utilization of up to 25 % formulated as a target, the economic savings through the reduced need for copper and electrical steel clearly outweigh the price increases due to the composite for winding insulation. With regard to large quantities such as in electric mobility, the Al_2O_3-filled system should be further developed. For high-performance applications such as in special machine construction or electric flying, the AlN or BN-filled system will be of interest.

IV. INVESTIGATION OF COMPOSITE SAMPLES OF INSULATION SYSTEMS

A. IMPREGNATION OF WINDING COMPOSITE SAMPLES

1) PRODUCTION OF THE COMPOSITE WINDING SAMPLES

Based on the results of the previously described material development and characterization, composite winding samples were constructed. These provided a basis for investigating the suitability of the ceramic-filled composite materials as impregnations for electrical windings. The wire bundles were

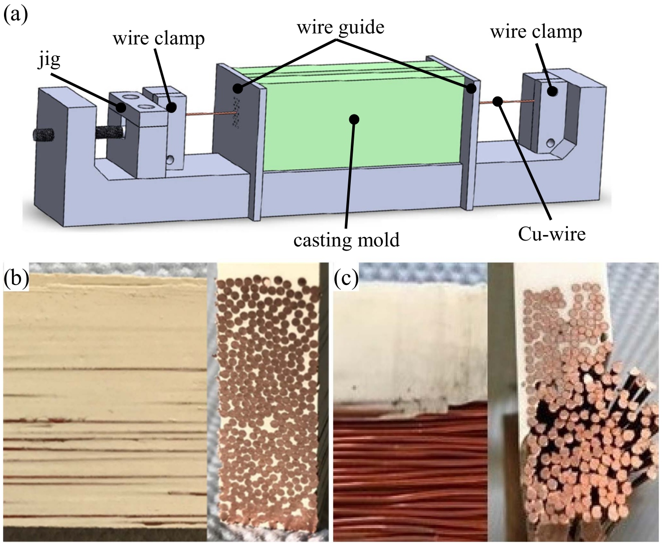

FIGURE 4. Production of composite winding samples. (Detail: (a) Wire tensioning device and casting mold; round wire winding with copper fill factor $\varphi_{Cu} \approx 57$ %, wire diameter $d_{Cu} = 0.85$ mm, grade 2 polyurethane insulation with wall thickness $b_{iso} = (28 \ldots 44)$ μm, (b) AlN- and (c) BN-based composite system.)

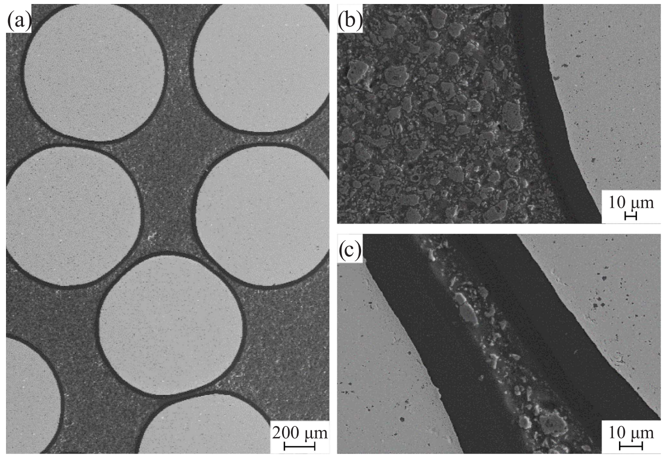

FIGURE 5. Microstructure analysis of the winding composite (AlN-filled impregnant. (a) Filler distribution. (b) Interface connection. (c) Wire gap filling).

pretensioned with the tensioning device shown in Fig. 4(a) and enclosed in a casting mold. Casting took place under vacuum (100 mbar) at 140 °C/1 h and subsequent crosslinking at 180 °C/8 h under normal pressure. With the Al_2O_3- and AlN-filled impregnation systems, the round wire winding was completely infiltrated [cf., Fig. 4(b)] whereas the BN-filled system showed insufficient infiltration due to the coarse filler [cf., Fig. 4(c)]. With regard to further investigations, the approach of filling with BN was not taken into account anymore. In addition to the round wire samples, composite samples were also built with flat wire (2.8×1.25) mm^2 with a copper fill factor $\varphi_{Cu} \approx 78$ %. A complete infiltration with the Al_2O_3- and AlN-filled impregnation was verified [28].

Additional composite winding samples based on state-of-the-art polyesterimide (PII) were also produced for comparative tests.

2) EXAMINATION OF COMPOSITE WINDING SAMPLES

In order to characterize the winding composite, grinding surface patterns were examined using the scanning electron microscope. Temperature change tests were carried out; the equivalent thermal conductivity was determined experimentally as well as calculated numerically.

Using the grinding surface patterns of the round wire winding examined with the scanning electron microscope, it was possible to prove that the winding composite was impregnated without air inclusions and that the ceramic filler grains were evenly distributed in the polymer matrix [cf., Fig. 5(a) and (b)]. The interface between the surface of the enameled copper wire and the impregnation shows complete wetting [cf., Fig. 5(b)]; ceramic filler grains were detectable even in the tight spaces between the wires [cf., Fig. 5(c)].

Cycle tests on the composite winding samples have been carried out to investigate the thermal cycling capacity of the composite winding. For this purpose, the temperature was varied in the range (-35 …165) °C, with a temperature change of only 3.3 K/min and a holding time in the final values of 15 min, thus, a complete heating or cooling of the samples could be assumed. During the test, the condition of the samples was checked optically approximately every 100 cycles. Small cracks and flakings were acceptable, the disintegration or break-up of the sample defines the defect of the specimen. During the first tests on the composite winding samples, no microscopy examination or measurement of the insulation resistance was carried out between the cycles. Starting from crack formations, the Al_2O_3-sample has been destroyed, whereas the sample with AlN filling and the one based on PII remain almost undamaged until the end of the test after 1735 cycles (cf., Fig. 6). In the real machine, the winding compound is stabilized by the electrical laminated core. With regard to further work, the thermal, electrical, ambient, and mechanical load capability (team factors) have to be examined in detail for the ceramic-like insulation system on motorettes.

The hot disk method, which was used to measure the specific thermal conductivity of the material samples, assumes spherical heat propagation in isotropic media [33] and can, therefore, not be applied to determine the equivalent thermal conductivity of the winding composite. The measurement was carried out using the heat flow measurement method according to Fig. 7. The test setup consisted of a Cu heating plate with three electrical resistors (power dissipation of 5 W each), the composite winding sample between two heat-flow-measuring plates and a Cu cooling plate with Al heat sinks. The individual layers were mounted applying a cover with heat-conductive paste ($\lambda \approx 10$ W/(m·K)), cf., Fig. 7(a). The joint gap is not influencing the measurement accuracy because the temperature probes are located directly on the probe surface. The stack was held together with a hard paper

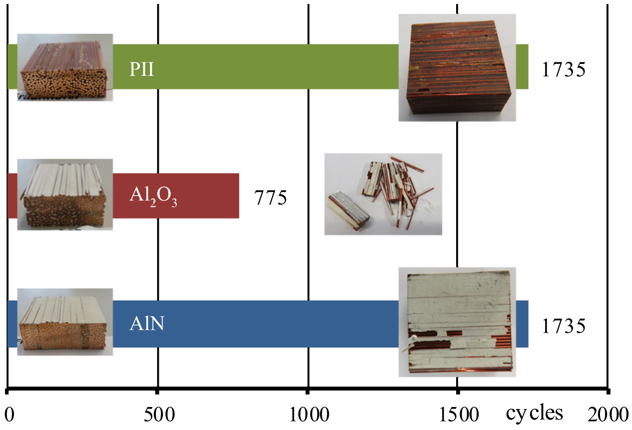

FIGURE 6. **Temperature cycle tests on composite winding samples (round wire winding with copper fill factor $\varphi_{Cu} \approx 57$ %, wire diameter $d_{Cu} = 0.88$ mm and insulation wall thickness $b_{iso} = 25$ μm; alternating thermal load over 1735 cycles in the range (-35 …165) °C with a temperature change rate of 3.3 K/min and a 15-min holding time in the final value).**

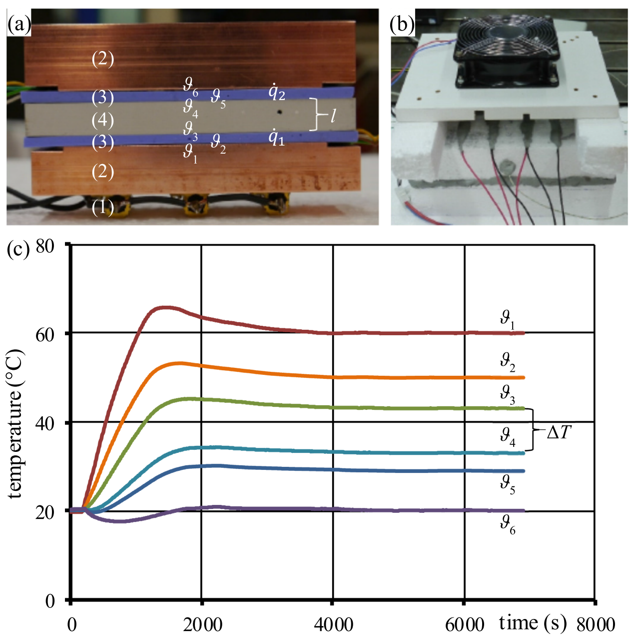

FIGURE 7. **Experimental determination of the equivalent thermal conductivity of the winding composite using the heat flow measurement method. (Detail: (a) Buildup of stack: (1) Resistors, (2) copper plate, (3) heat flow measuring plate with temperature sensor, (4) AlN-sample and (not shown) heatsinks mounted with heat-conductive paste. (b) Insulation of test setup and auxiliary fan. (c) Exemplary temperature curves at the measuring points of the stack structure of the AlN-sample).**

frame; 150 mm thick Styrofoam plates were used for thermal insulation and cooling was provided by an auxiliary fan [see Fig. 7(b)]. In the stationary thermal state [cf., Fig. 7(c)], the mean values of the measured heat flow densities $\dot{q}$, the temperature difference over the test sample measured with thermocouples $\Delta T = \vartheta_3 - \vartheta_4$ and the sample thickness l resulted in the calculation of the equivalent thermal conductivity

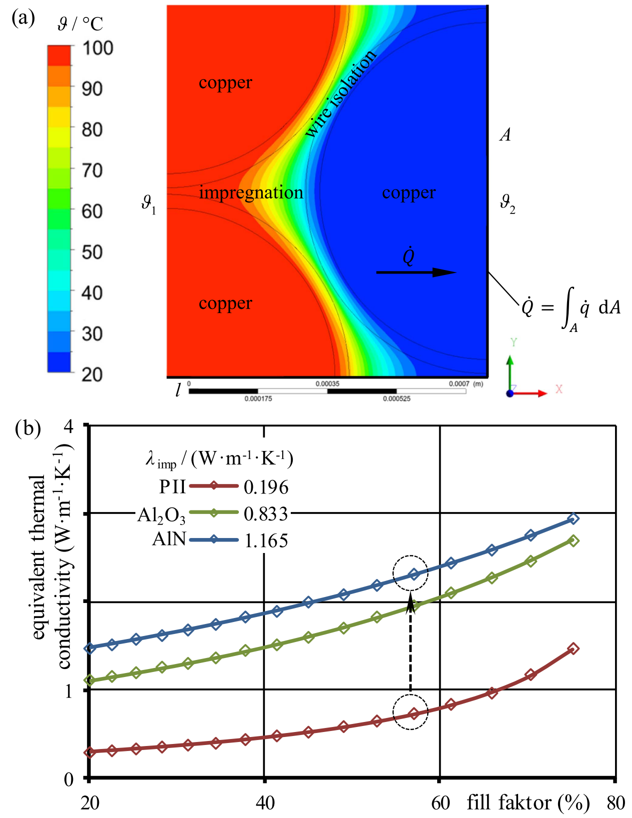

FIGURE 8. **Numerical analysis of the equivalent thermal conductivity of the winding compound. [Enameled copper wire: Wire diameter $d_{Cu} = 0.85$ mm, thermal conductivity of copper $\lambda_{Cu} = 385$ W/(m·K), insulation wall thick-ness $b_{iso} = 25$ μm and thermal conductivity of insulation $\lambda_{iso} = 0.2$ W/(m·K)].**

of the winding compound based on the equation

$$\lambda_{exp} = \frac{1}{2} \cdot \frac{(\dot{q}_1 + \dot{q}_2) \cdot l}{\vartheta_3 - \vartheta_4}. \quad (1)$$

For the winding composite impregnated with the AlN-filled material, an equivalent thermal conductivity of 1.57 W/(m·K) was measured; for Al_2O_3-filling of the polymer matrix a value of 1.38 W/(m·K) was determined. However, measurements on homogeneous samples of the pure impregnation materials show relative deviations of up to -30 % compared to the hot disk method. Consequently, higher thermal conductivities than the measured ones can also be expected for the composite samples.

For comparison with the experimental values, the equivalent thermal conductivity of the winding compound was also calculated numerically. For an orthocyclic wire arrangement shown in Fig. 8(a), the thermal conductivity of the impregnation and the copper fill factor were varied with constant parameters of the enameled copper wire (changing the geometric model dimensions). With the heat flow $\dot{Q}$ calculated by integration, the length of the heat conduction path l, the permeated area A, and the temperature difference $\Delta T = \vartheta_1 - \vartheta_2$, the equivalent thermal conductivity of the winding compound

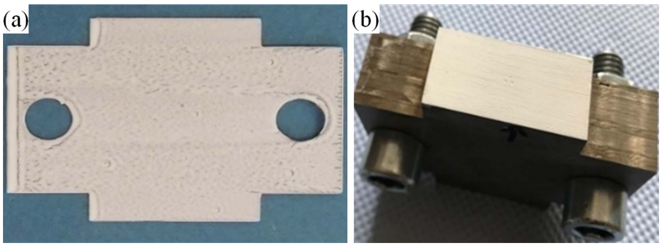

FIGURE 9. Production of electrical sheet composite samples. (Detail: (a) Electrical sheet with AlN dip coating with a layer thickness of $b_{iso} = 0.1$ mm. (b) Lamination stack with AlN brush coating of layer thickness $b_{iso} = 0.16$ mm).

can be calculated with

$$\lambda_{equ.wt} = \frac{\dot{Q} \cdot l}{A \cdot (\vartheta_1 - \vartheta_2)}. \quad (2)$$

By increasing the thermal conductivity of the impregnation, the equivalent thermal conductivity of the winding compound can be significantly increased. For example, in analogy to the constructed composite winding samples, impregnation with polyesterimide results in an equivalent thermal conductivity of $\lambda_{equ.wt.PII} = 0.71$ W/(m·K), whereas with AlN filling of the impregnating material $\lambda_{equ.wt.AlN} = 2.30$ W/(m·K) can be achieved, which corresponds to a relative increase in the thermal conductivity of the winding compound of 224 % [see Fig. 8(b)]. In comparison with the measured values from the heat flow measurement method, there is a relative deviation of the measurement of -31 %. Thus, the experimental setup of the heat flow measurement method is to be analyzed with regard to a systematic error at a later stage. Ongoing, the calculation results of the numerical model are used to describe the orthotropic thermal conductivity of the winding composite in the thermal models.

B. DIP COATING OF ELECTRICAL SHEET COMPOSITE SAMPLES

1) PRODUCTION OF ELECTRICAL SHEET COMPOSITE SAMPLES

As explained earlier, conventional insulating sheet materials for the main insulation of the lamination stack have specific thermal conductivities of < 0.2 W/(m·K), which results in a large temperature gradient between the electrical winding and the lamination stack. With the aim of realizing a thin insulation layer with good thermal conductivity and an improved interface connection between the winding impregnation and the main insulation, the ceramic-like composite system is to be modified in such a way that it is suitable for the dip coating of electrical laminated cores. To investigate the dielectric strength and thermal cycling capacity, composite samples were produced in the form of coated individual sheets of type M400-50A and coated stacks of sheets (cf., Fig. 9). The coating was applied to the individual sheets by dipping and to the sheet stacks by brushing. The stacks were heated to 120 °C. Additions of thixotropic agents such as Ultrasil VN3 in the range of (0.5 …2) ma.-% allowed for adjusting the layer thickness for a single dipping in a range of (0.05 …0.5) mm. At the same time, an attempt was made to coat lamination stacks using the injection molding process, with the insulation wall thickness being (0.5 …2) mm. However, poor adhesion of the insulation layer was found. The cause are antiadhesive additives in the injection molding system, which form rigid polymer structures during crosslinking. An adjustment of the thermal expansion coefficient of the ceramic-like insulation system would be necessary. Regarding the technologically simpler dipping process, injection molding technology was not pursued further for the time being.

2) EXAMINATION OF ELECTRICAL SHEET COMPOSITE SAMPLES

For an initial characterization of the ceramic-like insulation layer on the electrical sheet, the dielectric strength was determined and the thermal cycling capacity was investigated.

To measure the dielectric strength of the ceramic-like insulating layer on the electrical sheet, the layer heights were first analyzed with a micrometer gauge, with the test sheets having an insulating wall thickness in the range of (0.06 …0.1) mm. To prevent creeping discharges on the surface of the insulating layer, the measurement was carried out in oil and with cylindrical electrodes with a diameter of 6 mm. The electrode was placed in the middle of the coated electrical sheet outside of the oil bath. Mechanical bracing of the electrode and the grounded electrical sheet prevented an additional oil film from forming between the sample and the electrode, which would positively falsify the measurement result. During the measurement, the voltage was increased at a rate of change of 2.5 kV/s and the breakdown voltage was recorded. The dielectric strength results from the quotient of the breakdown voltage and the insulation wall thickness. Measured values were around 30 kV/mm, which can be assessed as sufficient for the insulation of an electrical machine with a rated voltage <1 kV and a desired insulating layer thickness of approximately (0.1 …0.2) mm. With regard to voltage peaks at inverter feeding, a sufficient insulating capacity is also to be expected.

Parallel to the thermal cycle tests on the composite winding samples (cf., Fig. 6), the thermal cycling capacity of the ceramic-like electrical sheet coating was examined under the same load conditions. This resulted in more stable behavior for the coating with the AlN-filled system compared to the Al_2O_3-filled system, with the electrical resistance of the AlN coating being even greater than 50 MΩ at the end of the investigation (cf., Fig. 10). In the future, the Al_2O_3-filled system should also be further optimized, since it will probably be 5–10 times cheaper than the AlN system.

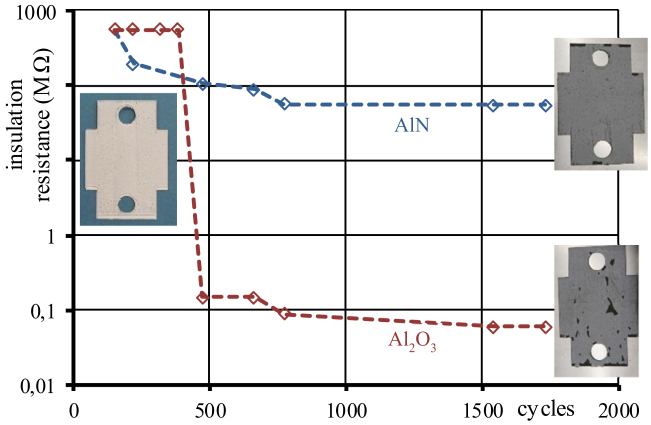

FIGURE 10. Temperature cycle tests on electrical sheet composite samples (electrical sheets with a ceramic-like dip coating with a layer thickness of $b_{iso} = 0.1$ mm; thermal cycling over 1735 cycles in the range (-40 …170) °C / 15 min holding time).

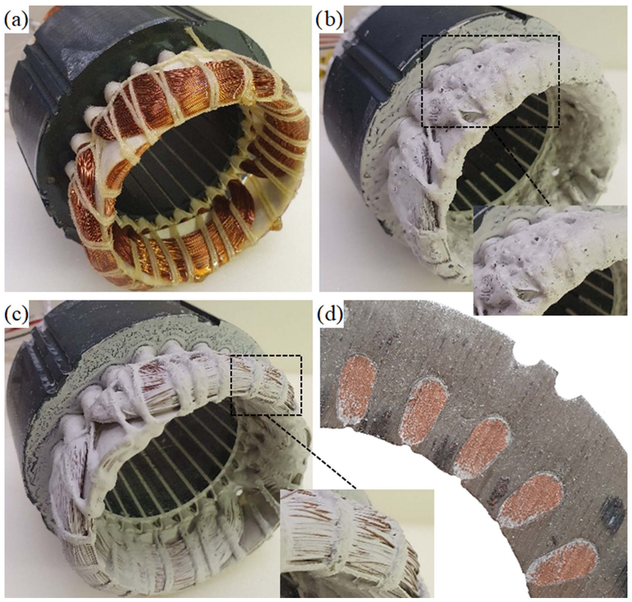

FIGURE 11. Production of test samples with PII and AlN impregnation and investigation of the production technology (IE3 induction machine (shaft height 63) with distributed winding (wire diameter $d_{Cu} = 0.265$ mm and copper fill factor $\varphi_{Cu} = 71.2$ %). (a) PII impregnation with styrene solvent. (b) Solvent-free AlN impregnation (40 vol.-%). (c) AlN impregnation (40 vol.-%) with solvent acetone (2 ma.-%). (d) Verification of the saturation in a destructive test by sawing (dimensions: Slot height $h_n = 9.5$ mm and slot width $b_n = 5.4$ mm).

V. INVESTIGATION OF PROCESSING TECHNOLOGY BASED ON TEST SAMPLES

A. IMPREGNATION OF WINDINGS

1) MANUFACTURING AND PROCESSING TECHNOLOGY

For the practical investigation of the production technology, stators of an IE3 standard induction machine of shaft height 63 were impregnated with the Al_2O_3- and the AlN-filled composite material, with conventional insulating sheets initially being used as the main insulation of the laminated core (cf., Fig. 11). The impregnation was carried out by slowly immersing the preheated stators in an immersion bath heated to 120 °C, subsequent venting at 100 mbar/2 h, removal from the immersion bath and final crosslinking at 180 °C/8 h. In the first tests, however, excess insulating material dripped off poorly at the winding overhangs [cf., Fig. 11(b)] and air inclusions in the slots were sometimes found in cutting samples. By adding up to 2 % by mass of acetone as a highly effective thinner for the impregnation, the impregnation, and ventilation time could be reduced by half. Excess material runs off the winding heads much better [cf., Fig. 11(c)] and for both the AlN and the Al_2O_3- filled composite system, it was possible to demonstrate complete soaking of the slots on the basis of cutting samples [cf., Fig. 11(d)].

2) INVESTIGATION OF THE IMPREGNATION

In addition to the abovementioned destructive cutting tests, the impregnation was assessed by means of partial discharge (PD) measurements, with stators conventionally impregnated on a PII basis also being examined for comparison purposes. With the test setup shown in Fig. 12(a), the measurements were carried out with sinusoidal supply in a high-voltage laboratory. When measuring according to DIN EN 60270, the feeding was carried out via a measuring transducer with a subsequent standard measuring circuit and measured value acquisition via a *LDS-6* and a *MPD 600* measurement system, respectively. When measuring the single winding phases against the grounded lamination stack, the polyesterimide-based standard impregnation resulted in a minimum PD inception voltage of 0.94 kV and the minimum PD extinction voltage was 0.76 kV. In comparison, the measurements of the AlN-filled system resulted in a minimum PD inception voltage of 0.98 kV and a minimum PD extinction voltage of 0.73 kV [cf., Fig. 12(c)]. As a result, no significant difference between the insulation systems could be determined. During the PD measurement of one winding phase against the two other winding phases connected to ground, the PD extinction voltages of both insulation system variants were approximately (300 …600) V higher than when measuring against the grounded lamination stack. From the phase resolved partial discharge plot shown in Fig. 12(b) and a similar amplitude can be determined for both half-waves, which indicates cavity discharges between the conductors. At the same time, PD measurements according to DIN EN 60034-18-41 were carried out by the motor manufacturer, whereby no significant differences could be determined compared to the standard insulation; the impulse voltage insulation class D (extreme stress) was verified with the standard-compliant test and indicates a good behavior under switched voltages from an inverter.

Initial heating tests were carried out on the impregnated test stators with a defined loss generation and cooling without forced convection. In comparison to the standard polyesterimide-based insulation, the mean excess temperature could be reduced by approximately 5 K based on an average excess winding temperature of 105 K with the AlN-filled

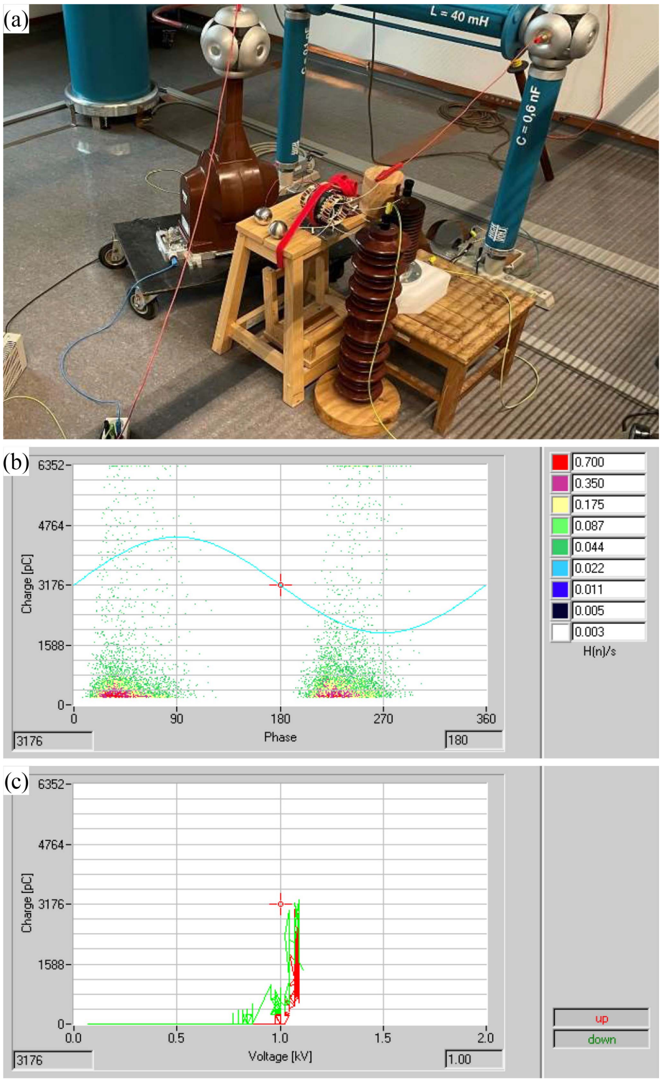

FIGURE 12. **Partial discharge measurements on test samples. (Detail: (a) Experimental setup in high-voltage laboratory, (b) phase resolved partial discharge pattern, (c) Inception and extinction voltage with sinusoidal power supply on test sample with AlN impregnation system.)**

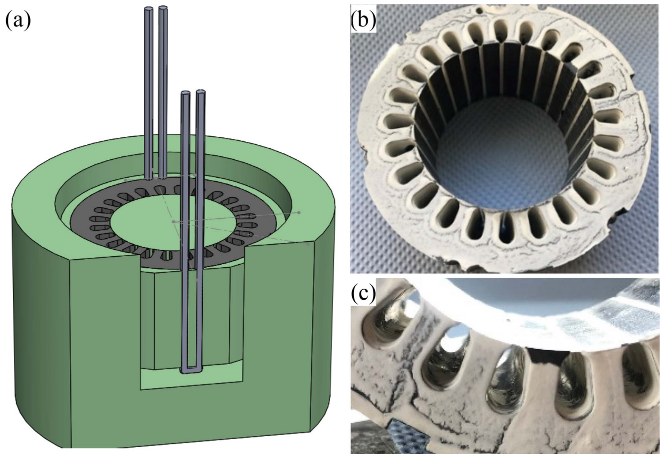

FIGURE 13. **Production of test samples with AlN dip coating as the main insulation of the laminated core and investigation of the production technology. (Detail: (a) Setup for dip coating. (b) Lamination stack IE3 induction machine (shaft height 63, outer diameter da = 96 mm, slot height hn = 9.5 mm, and slot width bn = 5.4 mm). (c) Uneven coating of the slot edges on the face of the laminated core.)**

impregnation and by approximately 3.5 K with Al_2O_3 filling, which already demonstrated a small advantage against the state of the art. When installed in a demonstrator machine and with a connection of the stator laminations to the heat-dissipating housing, a significantly greater reduction in the excess winding temperature can be expected (cf., Section VI).

B. DIP COATING OF LAMINATION STACKS

The suitability of the insulating materials for applying the main insulation in a dipping process was also examined on the lamination stack of the test sample (induction machine, shaft height 63). The thixotropic AlN-filled composite system was heated to 120 °C, the laminated core was immersed and slowly lifted out of the coating mass [cf., Fig. 13(a)]. The subsequent crosslinking of the insulating layer took place at 180 °C/8 h. The result was an uneven layer formation in the slots, which could not be improved even by prior cleaning of the slot surfaces so far. Likewise, layer interruptions at the edges were determined [cf., Fig. 13(b) and (c)]. A dependency on the slot dimensions and the previous laminated core production process was found; for example larger slot surfaces and baked laminated cores allow for a better coating. Additional edge protection in the form of an insulating plate is currently required on the end faces of the laminated core. The ceramic-like coating material and technology are to be further optimized in future research work. For example, a multistage coating process is conceivable to improve edge protection. In the first stage, a very thin, flexible, and firmly adhering layer is to be applied to the slot surface using a particularly low-viscosity composite system, and in the second stage, the mechanical edge protection is realized with a more thixotropic coating material.

VI. INVESTIGATION OF POTENTIAL FOR ENERGY EFFICIENCY AND POWER DENSITY INCREASE

A. MANUFACTURING OF DEMONSTRATOR MACHINES

Based on the results of experimental investigations on demonstrator machines, the potential for increasing the energy efficiency or the power density of electrical machines when using the new materials and processes for the winding insulation should be shown. On the one hand, an industrial induction machine, which underlies the energy efficiency classification, was built using the test stator with ceramic-like impregnated winding [cf., Fig. 14(a)]. On the other hand, a prototype of an outer rotor traction machine (modified for the test bench) was designed based on a concept study of a wheel hub drive for an electric motorcycle [see Fig. 14(b)]. The lamination stack of the traction motor is coated with a ceramic-like main insulation applied in a dipping process and the tooth coil

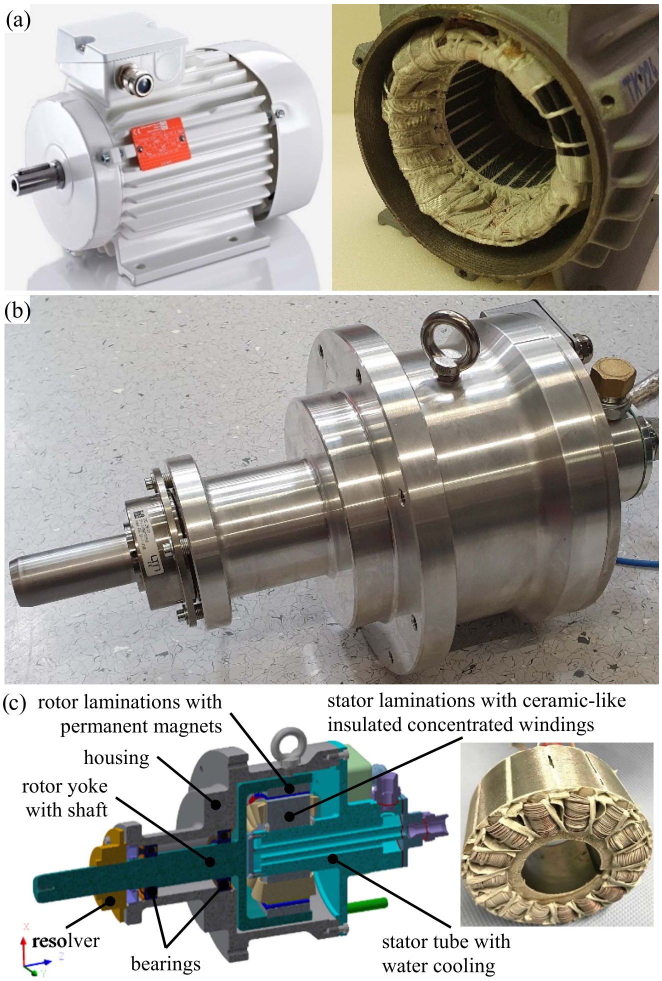

FIGURE 14. Demonstrator machines for investigating the energy efficiency and power density increase. [Detail: (a) IE3 induction machine (shaft height 63), (b) traction machine prototype, and (c) internal structure of permanent magnet excited outer rotor machine for traction applications with ceramic-like AlN-based winding insulation and internal cooling of the stator tube (main dimensions: inner stator diameter d_{si} = 45 mm, outer stator diameter d_{sa} = 104.4 mm, active length l_{Fe} = 43 mm, no. of stator slots N_s = 15 and number of poles $2p$ = 10)]

winding was impregnated with the AlN-filled composite system [cf., Fig. 14(c)]. For improved edge insulation, a 0.5 mm thick glass fiber plate is currently applied to the end faces of the laminated core. This results in an increase in phase resistance of 5.7 % compared to the conventionally insulated design due to the increase in the length of the end winding. For better comparability, both demonstrator machines were also set up with a standard insulation system (i.e., main insulation from polyester insulating sheet, impregnation polyesterimide based).

B. DESIGN OF THE WHEEL HUB TRACTION MACHINE

To determine the main dimensions and the winding design of the machine, an electromagnetic design case study was per formed at IAV applying JMAG-Designer. The electromagnetic optimization as well as the design of the internal stator

TABLE 3. Performance Data and Separation of Losses in Operating Points

Property	Continuous power point	Max. power point
operation mode	S1	S2 - 20 s
mechanical power P_2 (kW)	9.47	23.06
average torque T (Nm)	12.5	30.4
mechanical speed n (r/min)	7244	7244
core loss stator tooth (W)	397.4	513.1
core loss stator back (W)	63.7	82.6
core loss rotor yoke (W)	0.5	0.5
loss magnets (W)	87.6	353.4
stranded loss slot (W)	133.6	950.0
stranded loss end winding (W)	64.4	457.5
mechanical loss (W)	150.6	150.6
total loss P_{loss} (kW)	0.90	2.51
efficiency η (%)	91.3	90.2
utilization C (kVA·min/m^3)	3.16	8.00
thermal load $A{\cdot}J$ (kA/m·A/mm²)	374	2661

tube cooling system were carried out at the university using the software packages ANSYS Maxwell and ANSYS CFX. Optimization calculations were accomplished regarding pole geometry/pole segmentation and air gap width with the aim of reducing eddy current loss in the magnets (further explanations on the electromagnetic and thermal design of the traction machine cf., [29]). The performance data and losses summarized in Table 3 result from the calculations for the operating points at continuous power and at maximum power and are independent of the choice of insulation system.

Based on the loss distribution and assuming constant boundary conditions, which were determined by means of additional equivalent models and a heat source network, the stator heating at the continuous power point was calculated for the different thermal conductivities of the insulating materials. With the conventional implementation of the winding insulation, the calculated maximum winding temperature $\vartheta_{w.max}$ is 166.5 °C [cf., Fig. 15(a)], the reference temperature being ϑ_{ref} = 40 °C. For the implementation of the winding insulation in thermal class H, there is a reserve for the maximum permissible winding temperature of 13.5 K. With the ceramic-like insulation system assumed in Fig. 15(b), the maximum winding temperature can be reduced by approximately 30 K, which corresponds to a relative change in the winding excess temperature $\Delta\vartheta_{w.ave}$ of -23,7 %. With the models presented, it was estimated in further calculations that the electromagnetic utilization at the continuous power point can be increased by approximately 15 %.

C. EXPERIMENTAL INVESTIGATION OF DEMONSTRATOR MACHINES

The experimental investigation of the demonstrator machines was carried out in the form of machine tests with a defined

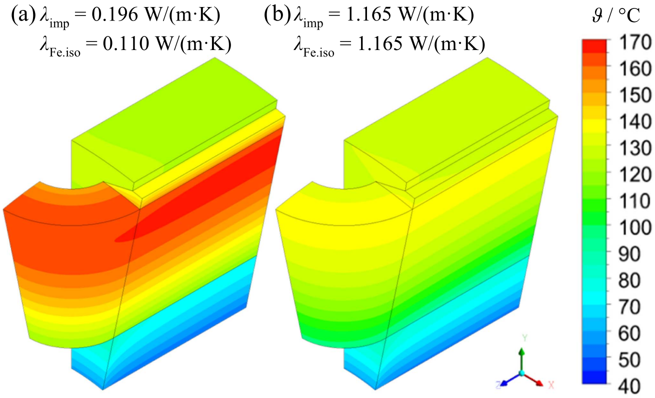

FIGURE 15. Calculation of the temperature distribution in the stator depending on the thermal conductivity of the insulation system. (Detail: (a) Standard insulation system and (b) ceramic-like insulation system; lamination stack: $\lambda_{Fe.t} = 24.8$ W/(m·K) and $\lambda_{Fe.n} = 0.9$ W/(m·K); stator winding: $\lambda_{Cu} = 385$ W/(m·K), $\varphi_{Cu.iso} = 59$ %, $d_{Cu} = 0.71$ mm, $\lambda_{iso} = 0.2$ W/(m·K), $b_{iso} = 52$ μm $\rightarrow$ $\lambda_{equ.wt.PII} = 0.78$ W/(m·K), $\lambda_{equ.wt.AlN} = 2.38$ W/(m·K) and $\lambda_{equ.wn} = 230$ W/(m·K); insulating sheets: $\lambda_{iso} = 0.11$ W/(m·K) and $b_{iso} = 0.4$ mm; air gap heat transfer: $\alpha_{\delta} = 60.3$ W/(m²·K) and $\Delta\vartheta_{f.\delta} = 84.2$ K; end winding heat transfer: $\alpha_{w} = 76.2$ W/(m²·K) and $\Delta\vartheta_{f.w} = 97.6$ K; cooling system heat transfer: $\alpha_{equ.c} = 16 \cdot 10^3$ W/(m²·K), $\vartheta_e = 30$ °C and joint gap $\delta_{iso} = 25$ μm).

load and cooling for the thermal steady state at selected operating points. Both for the IE3 induction machine (shaft height 63) and for the outer rotor traction machine, two versions with a conventional insulation system (insulating sheets as the main insulation of the lamination stack and polyesterimide-based impregnation of the stator winding) and a ceramic-like AlN-based insulation system according to Fig. 14 were examined in comparison.

At the rated point of the induction machine, the average winding excess temperature $\Delta\vartheta_{w.ave}$ measured using the resistance measurement method is only 29.2 K for the version with standard insulation, whereby a winding excess temperature of 105 K would be permissible for the version with thermal class F. This clearly shows that in the case of machines of small size, a significant reduction in electromagnetic utilization is necessary to achieve the required energy efficiency, which results in a deterioration in resource efficiency (approximately (5 …10) % increase in active mass per percentage point increase in efficiency). At the same load, the improvement in heat dissipation from the winding with the ceramic impregnation results in a temperature reduction of 5.3 K, which corresponds to a relative change of -18.2 %. As a result of the reduction in winding resistance and the resulting reduction in Joule losses, there is an increase in efficiency of 1.3 % (cf., Table 4). In addition, operating points in the overload range up to 2.3 times the rated power were examined, which resulted in a maximum relative change in the average winding temperature of up to -37 % with an associated increase in efficiency of 6.8 % for the standard induction machine with ceramic-like insulation.

Especially for drives in mobile applications, a high power density is desired with the aim of reducing mass, which is

TABLE 4. Comparison of Results of Experimental Investigation of Standard Industrial Induction Machine in Selected Operating Points

Insulation	U_{LL} (V)	I_L (A)	$\cos\varphi$	P_1 (W)	n (rpm)	T (Nm)	P_2 (W)	η (%)	$\Delta\vartheta_{w.ave}$ (K)
standard (PII)	400	0.37	0.74	189	1395	0.82	120	**63.6**	**29.2**
	480	0.60	0.86	428	1264	1.81	240	**56.0**	**84.9**
ceramic-like (filler AlN)	400	0.36	0.75	185	1399	0.82	120	**64.9**	**23.9**
	480	0.58	0.85	405	1294	1.77	240	**59.3**	**64.1**

Red stands for the warmer starting system and Green shows the improved system.

TABLE 5. Comparison of Results of Experimental Investigation of Traction Drive in Selected Operating Points

Insulation	U (V)	I (A)	P_1 (kW)	n (rpm)	T (Nm)	P_2 (kW)	η (%)	$\Delta\vartheta_{w.max}$ (K)	$\Delta\vartheta_{w.ave}$ (K)
standard (PII)	92.4	21.4	2.19	1500	12.6	**1.98**	**90.1**	**82.4**	**69.7**
	153.5	21.9	4.25	3000	12.6	**3.95**	**93.0**	**87.6**	**74.9**
ceramic-like (filler AlN)	94.9	20.8	2.19	1500	12.7	1.99	**90.8**	**36.3**	**29.6**
	96.9	30.2	3.28	1500	18.1	**2.85**	87.0	81.2	65.2
	158.1	21.5	4.27	2999	12.7	3.99	**93.5**	**44.2**	**37.3**
	160.2	30.5	6.14	3000	17.9	**5.64**	91.8	88.1	72.4

Red stands for the warmer starting system and Green shows the improved system.

essentially achieved by increasing the linear current density or the speed. Based on comparative measurements of the outer rotor traction machine, the potential for increasing the power density by increasing the linear current density, which is made possible by the improved heat dissipation when using ceramic-like insulating materials, should be demonstrated. The machines have Pt100 temperature sensors to determine the winding temperatures in the hot spots of the end windings, the mean winding temperature was determined using the resistance measurement method. Initially, two operating points were examined at continuous torque and the two speeds of 1500 rpm and 3000 rpm due to speed limitations of the test bench (cf., Table 5). For the machine with conventional insulation, there is a maximum winding excess temperature $\Delta\vartheta_{w.max}$ of 87.6 K at the end winding on the connection side and the mean winding excess temperature $\Delta\vartheta_{w.ave}$ is 74.9 K. Based on the permissible temperatures of the winding design in thermal class H, there is an excess temperature reserve of approximately 50 K. In the operating range of the base speed up to 7244 rpm, no impermissible heating of the machine is to be expected, despite increasing core loss and additional loss. At the operating points examined, the maximum winding excess temperature can be reduced by approximately 45 K and the average winding excess temperature by approximately 40 K by means of the innovative, ceramic-like insulation system (relative excess temperature changes in the range (49 …58) %). With the lower resistance of the stator winding at steady-state and the resulting lower Joule loss, there is an increase in efficiency of up to 0.75 %. At the investigated operating points, a relative increase in power density of up to 44% was experimentally proven with comparable maximum winding heating for the machine with ceramic-like winding insulation. Simultaneously, the higher electromagnetic utilization and higher power density result in an increased share of the Joule loss in the total loss and, thus, a reduction in efficiency by up to 3 % in comparison to the standard insulation system. The predicted power density increase of 15 % estimated for the continuous power point (base speed) using the numerical calculation model in Fig. 15 appears to be feasible easily on the basis of the results obtained so far. As part of further work, the investigation of the operating parameters in the entire speed-torque range is planned.

VII. CONCLUSION

The electromagnetic utilization of electrical machines is limited with regard to the maximum permissible temperature rating of conventionally used winding insulation materials. Furthermore, these materials only have low specific thermal conductivities of approximately 0.2 W/(m·K). As an alternative, the development and fundamental characterization of ceramic-like composite systems based on filled polysiloxanes were presented in the article and the suitability for isolating electrical windings was demonstrated in principle.

Due to the ceramic fillers, the specific thermal conductivity of the composite can be increased to a value of approximately 1 W/(m·K), whereby the simultaneously low viscosity still allows the impregnation of round and flat wire windings even with a high copper fill factor. By adding small amounts of acetone as a highly effective impregnation thinner, the impregnation and ventilation time could be reduced to approximately 1 h. The crosslinking time is currently 8 h at 180 °C, this shall be further reduced to around 2 h by optimizing the crosslinking catalyst. As a result, the equivalent thermal conductivity for the winding composite, consisting of enameled copper wire and ceramic-like impregnation, is two to three times higher than the state of the art.

Parallel to the development of impregnating materials, attempts were made to modify the ceramic-like composite system by adding thixotropic agents in such a way that it is suitable for dip-coating electrical laminations in order to achieve a thinnest possible and most heat-conducting main insulation. Dielectric strength of up to approximately 30 kV/mm, with adjustable layer thicknesses in the range of (0.05 …0.5) mm, could be demonstrated on single steel sheets. With regard to the dip coating of complete lamination stacks, an uneven layer height can still be determined, particularly with small slot dimensions, and the edge coating at the front sides must be assessed as critical. Additional edge protection is currently required. In further work, development approaches such as multiple coating with variation of the degree of thixotropy of the composite are to be examined.

Based on the experimental comparative study of a highly utilized permanent magnet excited synchronous machine for use in electric mobility, it has already been demonstrated that the ceramic-like insulation system can reduce the winding temperature by up to 58 % compared to conventional insulation, and thus, the power density can be increased by up to 44 %. With regard to the application of ceramic-like insulating materials for the insulation of electrical machines, further R&D work will be necessary. It should focus on the detailed investigation of the thermal, electrical, ambient, and mechanical stressability of the ceramic-like insulating system as well as the improvement of process reliability in the production of ceramic-like insulated lamination stacks. With regard to a broad applicability on the market, the further development of the composite system with Al_2O_3 filling should be focused from an economic point of view, since the AlN filler, which is up to ten times more expensive, will rather be suitable for high-performance applications. At present, the use of enameled copper wire still limits the thermal conductivity of the winding composite and its ability to withstand thermal stress. This results in a need for the development of ceramic-like conductor insulation.

REFERENCES

[1] M. Popescu, D. A. Staton, A. Boglietti, A. Cavagnino, D. Hawkins, and J. Goss, "Modern heat extraction systems for power traction machines—A Review," *IEEE Trans. Ind. Appl.*, vol. 52, no. 3, pp. 2167–2175, May/Jun. 2016.

[2] A. Fatemi, D. M. Ionel, M. Popescu, Y. C. Chong, and N. A. O. Demerdash, "Design optimization of a high torque density spoke-type PM motor for a formula E race drive cycle," *IEEE Trans. Ind. Appl.*, vol. 54, no. 5, pp. 4343–4354, Sep./Oct. 2018.

[3] C. Dong, Y. Qian, Y. Zhang, and W. Zhuge, "A review of thermal designs for improving power density in electrical machines," *IEEE Trans. Transp. Electrific.*, vol. 6, no. 4, pp. 1386–1400, Dec. 2020.

[4] T. Epskamp, "Steigerung der leistungsdichte von traktionsantrieben und aufbau einer hochdrehenden asynchronmaschine," Ph.D. dissertation, Karlsruher Instituts für Technologie, Karlsruhe, Germany, 2020.

[5] P. Harnisch et al., "Optimized manufacturing process and modelling of squirrel-cage induction machines with copper cage and axially segmented end rings for high-speed applications," in *Proc. 10th Int. Electric Drives Prod. Conf.*, 2020, pp. 1–8.

[6] D. Schmitz et al., "Design and test of squirrel cage induction machines with high power density, cast copper cage and high-strength low-loss NGO-electrical steel," in *Proc. 11th Int. Conf. Electric Veh. Drives E-Mobility*, 2019, pp. 1–7.

[7] U. Schuffenhauer et al., "Realization of high-speed cast copper cage induction machines for electric mobility," in *Proc. 25th Int. Conf. Elect. Machines*, 2022, pp. 2290–2296.

[8] F. Herget et al., "Efficiency and power density improvement of squirrel-cage induction machines with cast copper cage and high strength electrical steel," in *Proc. 14th Int. Conf. Electric Veh. Drives E-Mobility*, 2022, pp. 1–8.

[9] S. Rost, "Vor- und Nachteile unterschiedlicher Verguss-Systeme (EP. PU. SI)," *3. Fachtagung E-Motoren und Transformatoren des Fachverbandes EWIS*, Fulda, Germany, Jan. 2013.

[10] C. Benedek, "Maßgeschneiderte PU-Vergussmassen und deren Zielkonflikte," *3. Fachtagung E-Motoren und Transformatoren des Fachverbandes EWIS*, Fulda, Germany, Jan. 2013.

[11] W. Hollstein, "Giessharzsysteme und Technologien für den Vollverguss des Stators bei Motoren und Generatoren," *3. Fachtagung E-Motoren und Transformatoren des Fachverbandes EWIS*, Fulda, Germany, Jan. 2013.

[12] M. C. Kulan, S. Şahin, and N. J. Baker, "An overview of modern thermo-conductive materials for heat extraction in electrical machines," *IEEE Access*, vol. 8, pp. 212114–212129, 2020.

[13] N. Simpson, P. H. Mellor, and R. Wrobel, "Estimation of equivalent thermal parameters of electrical windings," in *Proc. 20th Int. Conf. Elect. Machines*, 2012, pp. 1294–1300.

[14] D. Cozonac, S. Babicz, S. Ait-Amar-Djennad, G. Velu, A. Cavalini, and P. Wang, "Study on ceramic insulation wires for motor windings at high-temperature," in *Proc. IEEE Conf. Elect. Insul. Dielectric Phenomena*, 2014, pp. 172–175.
[15] D. Cozonac et al., "Materials characterization and geometry of a high temperature induction machine," in *Proc. 21st Int. Conf. Elect. Machines*, 2014, pp. 2499–2505.
[16] N. Zouzou, T. T. Dang, S. Duchesne, G. Vélu, and O. Ninet, "Modeling and experimental characterization of nickel-coated copper wires for the design of extremely high-temperature electrical machines," *IEEE Trans. Magn.*, vol. 56, no. 3, Mar. 2020, Art. no. 6100209.
[17] D. Malec, D. Roger, and S. Duchesne, "An electrical machine made with inorganic rigid coils: A breakthrough toward high temperature motors designed for aeronautics," in *Proc. IEEE 36th Elect. Insul. Conf.*, 2018, pp. 1–4.
[18] V. Iosif et al., "Technological assessments for designing machines able to work at very high internal temperatures (450–500 °C)," in *Proc. 22nd Int. Conf. Elect. Machines*, 2016, pp. 2682–2687.
[19] C. Weber and F. Liebetrau, "Investigation of ceramic-coated profile conductors regarding insulation strength with the aim of better thermal connection to the laminated core of electrical machines," in *Proc. 12th Int. Electric Drives Prod. Conf.*, 2022, pp. 1–5.
[20] W. Yin et al., "Highly thermally conductive insulation for high power density electric machines," in *Proc. AIAA/IEEE Electric Aircr. Technol. Symp.*, 2019, pp. 1–7.
[21] W. Übler, "Enhancement of the thermal conductivity of electrically insulating polymer materials," Ph.D. dissertation, Friedrich-Alexander-Universität Erlangen-Nürnberg, Technische Fakultät, Erlangen, Germany, 2002.
[22] T. Tanaka, G. C. Montanari, and R. Müllhaupt, "Polymer nanocomposites as dielectrics and electrical insulation-perspectives for processing technologies, material characterization and future applications," *IEEE Trans. Dielectrics Elect. Insul.*, vol. 11, no. 5, pp. 763–784, Oct. 2004.
[23] X. Huang, P. Jiang, and T. Tanaka, "A review of dielectric polymer composites with high thermal conductivity," *IEEE Elect. Insul. Mag.*, vol. 27, no. 4, pp. 8–16, Jul./Aug. 2011.
[24] T. Tomášková and P. Trnka, "The influence of thermal properties of aluminum oxide on electrical insulating materials," in *Proc. 15th Int. Sci. Conf. Electric Power Eng.*, 2014, pp. 421–425.
[25] T. Tomášková, R. Pechanek, and V. Kindl, "Benefits of upgrading insulating materials to operating temperature of induction motor," in *Proc. 17th Eur. Conf. Power Electron. Appl.*, 2015, pp. 1–6.
[26] T. Tomášková, A. Shlykevich, J. Hornak, P. Trnka, and M. Gutten, "The high voltage electrical insulation systems with higher thermal conductivity," in *Proc. IEEE Int. Conf. Dielectrics*, 2016, pp. 938–941.
[27] J. Samek, C. Ondrusek, and J. Kurfurst, "A review of thermal conductivity of epoxy composites filled with Al_2O_3 or SiO," in *Proc. 19th Eur. Conf. Power Electron. Appl.*, 2017, pp. 1–6.
[28] S. Miersch et al., "Ceramic-like composite systems for winding insulation of electrical machines," in *Proc. 24th Int. Conf. Elect. Machines*, 2020, pp. 1540–1546.
[29] S. Miersch et al., "Keramikähnliche kompositsysteme für die wicklungsisolation elektrischer maschinen," in *Freiberger Kolloquium Elektrische Antriebstechnik*, vol. 72. Freiberg, Germany: BHT-Freiberger Universitätsforum, 2021.
[30] R. Schubert et al., "Entwicklung und Analyse Polymer-Keramischer Isoliersysteme für die Wicklungsisolation energieeffizienter und hochausgenutzter elektrischer Maschinen," in *Fachtagung Polymere Isolierstoffe in der Elektrotechnik*, 2021, pp. 1–6.
[31] S. Miersch et al., "Investigation of ceramic-like composite systems for the winding insulation of a permanent magnet excited synchronous machine in outer rotor construction for an electric vehicle drive," in *Fachtagung VDE Antriebssysteme*, 2021, *Proc. Electromechanical Drive Syst., ETG Sympos.*, pp. 206–211.
[32] R. Schubert, *Entwicklung Funktionalisierter polymerkeramischer Komposite*. Hermsdorf, Germany: Fraunhofer-Institut für Keramische Technologien und Systeme, 2018.
[33] P. Krupa and S. Malinaric, "Using the transient plane source method for measuring thermal parameters of electroceramic," *Int. J. Mech. Mechatron. Eng.*, vol. 8, no. 5, pp. 735–740, Apr. 2014.
[34] A. Boglietti, A. Cavagnino, and D. A. Staton, "Determination of critical parameters in electrical machine thermal models," *IEEE Trans. Ind. Appl.*, vol. 44, no. 4, pp. 1150–1159, Jul./Aug. 2008.
[35] L. Idoughi, X. Mininger, F. Bouillault, L. Bernard, and E. Hoang, "Thermal model with winding homogenization and FIT discretization for stator slot," *IEEE Trans. Magn.*, vol. 47, no. 12, pp. 4822–4826, Dec. 2011.

SÖREN MIERSCH was born in Sebnitz, Germany, in 1980. He received the M.Sc. degree from Dresden University of Applied Sciences, Dresden, Germany, in 2008 and the Dr.-Ing. degree from Dresden University of Technology, Dresden, Germany, in 2020, both in electrical engineering.

He is currently a Postdoc in the field of electrical machines with the Department of Electrical Engineering, University of Applied Sciences Dresden. His research interests include the thermal and electromagnetic design of electric machines and drives.

RALPH SCHUBERT was born in Merseburg, Germany, in 1965. He received the Dipl.-Chem. degree in physical chemistry from the State University of Saint Petersburg, Saint Petersburg, Russia, in 1988.

From 1988 to 1992, he was a Scientific Assistant with the Department of Solid State Chemistry, Friedrich Schiller University, Jena. He moved to the Hermsdorfer Institute für Technische Keramik e.V. in Hermsdorf, Germany, in 1993, which was integrated into the Fraunhofer Institute of Ceramic Technologies and Systems in 2009. In the competence center for composite materials there, he is responsible for developing inorganic-organic composite materials, their processing by plastic forming techniques and their industrial applications.

THOMAS SCHUHMANN (Member, IEEE) was born in Schlema, Germany, in 1982. He received the Dipl.-Ing. degree in electrical engineering from Chemnitz University of Technology, Chemnitz, Germany, in 2005 and the Dr.-Ing. degree from Dresden University of Technology, Dresden, Germany, in 2011, in electrical engineering.

Since 2010, he has been with Siemens AG, Business Unit Large Drives, Nuremberg, Germany in the development department for high power electrical machines. In 2013, he was with IAV GmbH, Chemnitz, Germany (E-traction department). Since 2016, he has been a Professor with Dresden University of Applied Sciences. His research interests include modeling, design, and control of electrical machines and drives.

Dr. Schuhmann is a member of VDE and VDI. He is a reviewer for IEEE Transactions on Magnetics, Electric Power Components and Systems Journal, *International Conference on Electrical Machines* amongst others. In 2007, he was with the recipient of the VDE ETG publication award.

MATHIAS LINDNER was born in Stollberg, Germany, in 1984. He received the Dipl.-Ing. and Dr.-Ing. degrees in electrical engineering from Chemnitz University of Technology, Chemnitz, Germany, in 2009 and 2018, respectively.

In 2007, he was with the Department of Electrical Design and Test Development, Devotek As, Kongsberg, Norway. Since 2016, he has been with IAV GmbH, Chemnitz, Germany in the division of Future Powertrain/E-Machine Design. His main research interests include the electromagnetic and thermal design and simulation of electrical machines and drive systems as well as investigations on magnetic materials.